

Groundwater Inrush Channel Detection and Curtain Grouting of the Gaoyang Iron Ore Mine, China

Keqiang He · Ronglu Wang · Wenfu Jiang

Received: 4 July 2011 / Accepted: 21 September 2012 / Published online: 2 October 2012
© Springer-Verlag Berlin Heidelberg 2012

Abstract The complex hydrogeological conditions of the Gaoyang Iron Mine area were responsible for two water inrush accidents that occurred during tunneling at the horizontal level of −245 m on August 17, 2000 and August 29, 2004. Borehole computerized tomography in the key areas of the mine and groundwater level monitoring data were used to identify the main underground hydraulic channel and its characteristics. A grout curtain, designed and emplaced based on the results of this study, was highly effective in reducing the groundwater levels in the mine area and amount of water pumped from the mine.

Keywords Computerized tomography · Grout curtain · Underground hydraulic channel · Water inrush accidents

Introduction

The Gaoyang Iron Mine area, which is located in the Linzi District of Zibo City in Shandong Province, is a contact metasomatism magnetite deposit of skarn ore (Fig. 1). The hanging wall of the ore body is mainly hornstone, followed by skarn and diorite alteration. The ore body footwall is

limestone, under which there is a diorite intrusion (Wang 2005). The mining depth is −210 to −290 m. The designed annual production is 150,000 metric tons (t). The complex hydrogeological conditions of the Gaoyang Iron Mine area were responsible for two water inrush accidents that occurred during tunneling at the horizontal level of −245 m on Aug. 17, 2000 and Aug. 29, 2004, which severely flooded the auxiliary shaft. These were mainly caused by karst water from the footwall that entered the mine through an area where the limestone was exposed in the roadway.

Groundwater still endangered safe mining at the −285 m level, since the essential prerequisites for a groundwater inrush accident (Li et al. 2006), the water source, the head potential of the source water and the channels, were still present. Comprehensive understanding of the hydrogeological conditions and the underground hydraulic channel was necessary to prevent future water inrush incidents. Cross-hole electromagnetic computer tomography (CT) was used, along with groundwater monitoring, to locate the main groundwater channel of the mining area and ascertain its size, and to identify relevant cavities and shattered fault zones, which together explain the hydraulic conductivity and aquifer abnormalities in the mining area.

K. He (✉)
Department of Civil Engineering, Qingdao Technological
University, Qingdao 266033, Shandong, China
e-mail: keqianghe@sina.com

R. Wang
China Institute of Water Resources
and Hydropower Research, Beijing 100038, China

W. Jiang
Shandong Building Materials Geological Exploration
Center of SINOMA, Jinan 250000, China

Hydrogeologic Analysis of the Gaoyang Iron Mine Area

Regional Hydrogeological Analysis

The Gaoyang mine is located in the Jinling anticline region near the end of the northeast anticlinal Jinling minor axis. The Jinling anticline area is a relatively independent hydrogeological unit belonging to the groundwater system of the Zibo basin (Zhang 1989), which illustrates the Ordovician groundwater system as well as the nature of its



Fig. 1 The location of Zibo City (Gaoyang Iron Mine) in China

water supply, flow direction, and discharge (Fig. 2). It is dominated by a thick layer of Ordovician limestone that hosts the magnetite ore deposits and is the main aquifer of the area. The country rocks are sandstone, shale, and intrusive diorite, which are aquitards. The geological cross-section of the southern portion of the Gaoyang iron mine is shown in Fig. 3. The hydrogeological conditions surrounding the iron mining area are described in Table 1. The structure of the hydrogeological unit of the Jinling anticline area is a semi-enclosed U-shape, which blocks off much of the Ordovician limestone water flow from the northern part of the Zibo basin.

There are three possible groundwater sources in the Ordovician limestone in the area: (1) about 20 km² of limestone exposed in a ring with two gaps separated by intrusive diorite, which is located at a higher level and directly intercepts infiltrating rainfall; (2) the diorite rock formation that adjoins the limestone is exposed in a 30 km² area where it can absorb infiltrating rainwater and then recharge the limestone through the contact zone; (3) the Wuhe River, which receives groundwater recharge from the discharge area of the Zibo basin, flows through the south of the mine area, and is in hydrologic contact with the limestone rock. Based on precipitation data from 1971 to 2000 in Zibo city, the average annual precipitation is 609.9 mm (Bao et al. 2009).

Hydrogeological Conditions in the Gaoyang Iron Mine Area

The Gaoyang iron mine is located in the northeast portion of the Jinling anticline area. The hydrogeological

conditions of the iron mine area are shown in Table 2 and Fig. 4. The Ordovician limestone aquifer is confined in the east and west by two compressive reverse faults, the Zhangdian fault and the Jinling fault. In the southeast, low-permeability diorite forms a boundary. The water infiltrating into the Ordovician limestone of Jinling anticline moves toward the northeast, providing a continuous water supply from the southwest to the Gaoyang mine. Under natural conditions before mining, the groundwater saturated the limestone without discharging at the surface. Mining at Gaoyang tapped the Ordovician limestone groundwater, forming an artificial well.

Cavities can be observed everywhere in the Gaoyang iron mine area. During the exploitation process, along with the drainage of the deposit, many cavities, gaps, and shattered zones were exposed. Rocks in the shattered zones were fractured and fragmented. The cavities were filled in various ways. Thus, the Ordovician limestone is subject to water inrush, mainly from the west and south, through permeable pathways that include karst dissolution features, connected cavity systems, and shattered fault zones, which cause water inrushes into the roadway when intersected by mining. Therefore, the top priority for water inrush prevention and treatment involves exploration and identification of groundwater inrush channels west and south of the mine area.

The main aquifers in the area are the Ordovician limestone aquifer and the Quaternary formation aquifer. The highest roof elevation of the sandy gravel confined aquifer in the Quaternary system is −8.09 m. The lowest bottom elevation is −136.65 m. The total thickness of the aquifer

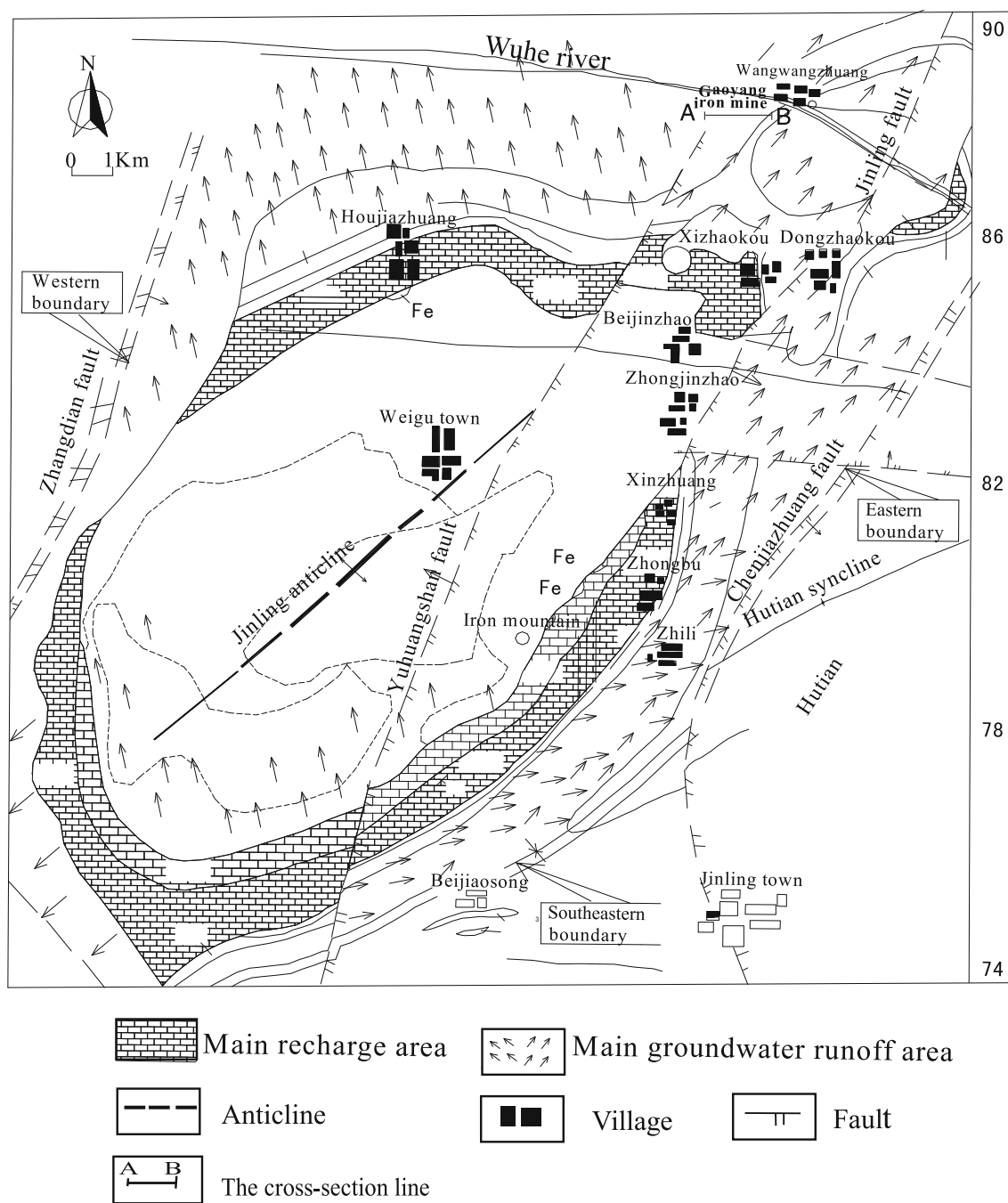


Fig. 2 Schematic groundwater movement (arrows) in the Ordovician limestone in Jinling mine area

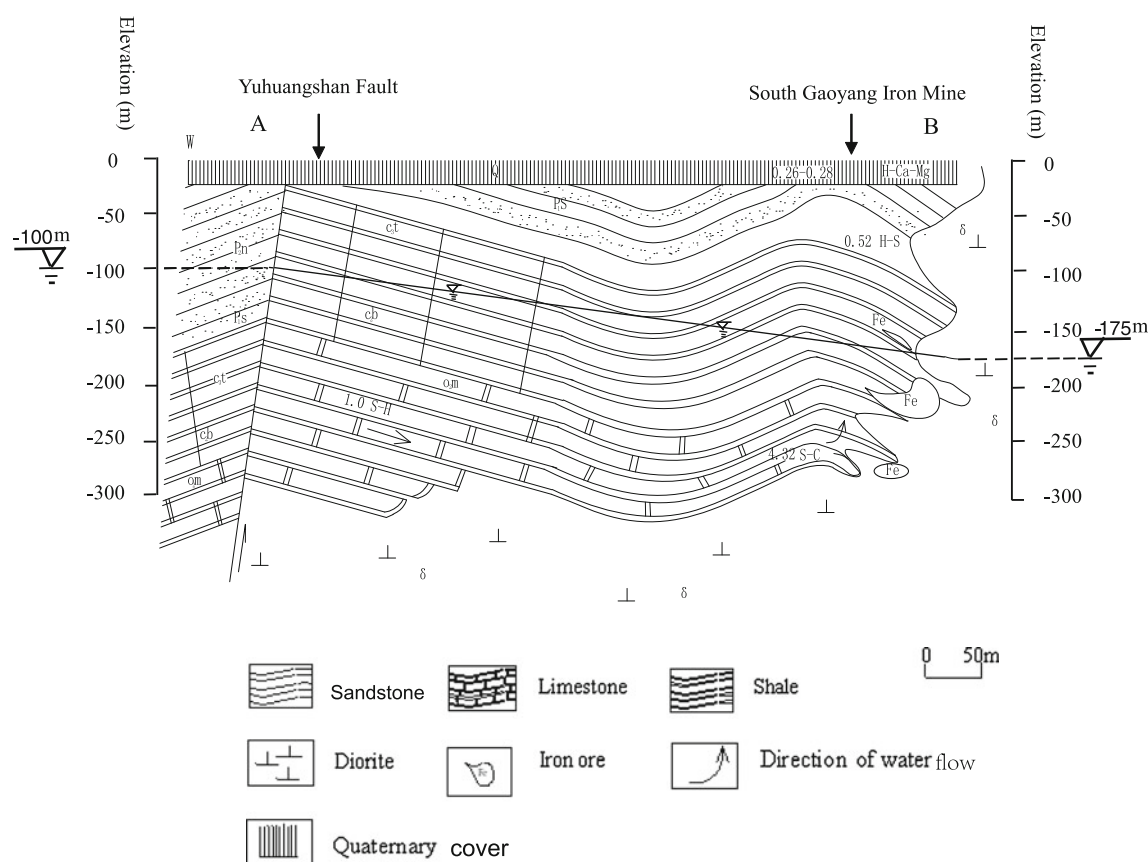
is between 8.88 and 43.55 m. The buried depth of groundwater is commonly 6 m or so, the water level elevation is between -266 and -268 m, and the hydraulic gradient is about 2.5 %. The buried depth of the roof of the Ordovician limestone is -347.18 to -576.57 m. The thickness of the Ordovician limestone ranges from a few meters to hundreds of meters.

The limestone layer in the Ordovician System serves as the major source of water for inrush events. Because a

virtually impermeable layer of clay has cut off the hydrodynamic connection of the Quaternary formation aquifer with this limestone aquifer, the groundwater level of the monitoring holes in the Quaternary formation aquifer has not been affected by the water inrushes and water drainage. Therefore, it can be concluded that the Quaternary formation aquifer was not connected with the water inrushes, and mining will not affect the groundwater of the Quaternary System in this region.

Table 1 Hydrogeological conditions of the Jinling anticline area

Boundary	Geologic structure	Hydrogeological conditions
West	Zhangdian fault	The Zhangdian fault is a compresso-shear reverse fault with a dip angle $>80^\circ$ and fault throw >800 m, resulting in no direct contact between the upper and lower zones of Ordovician limestone, which constitutes a water-resistant boundary west of the Jinling anticline area
East	Chen Jiazhuang fault	A water barrier is formed by the compresso-shear fault and Chen Jiazhuang fault
Southeast	Hutian syncline	The Ordovician limestone at the axis was emplaced deeper and the fissures and cracks of the Ordovician limestone are not developed on the north side. Also, this syncline has very limited porosity and permeability. Therefore, the Hutian syncline serves as a groundwater barrier to the southeast of the mine area by blocking the Ordovician underground water of the Zibo basin
North	Limestone	The limestone of the Gaoyang deposit is more than 300 m deep, extends more than 1000 m to the north, and is covered by Permian carbonic rock as the confining bed. Thus, the Jinling anticline area is enclosed, minimizing water supply in the northern part of the Gaoyang iron mine area

**Fig. 3** Hydrogeological cross-section of the south Gaoyang Iron Mine

Electromagnetic CT Detection for Groundwater Inrush Channels of Gaoyang Iron Mine

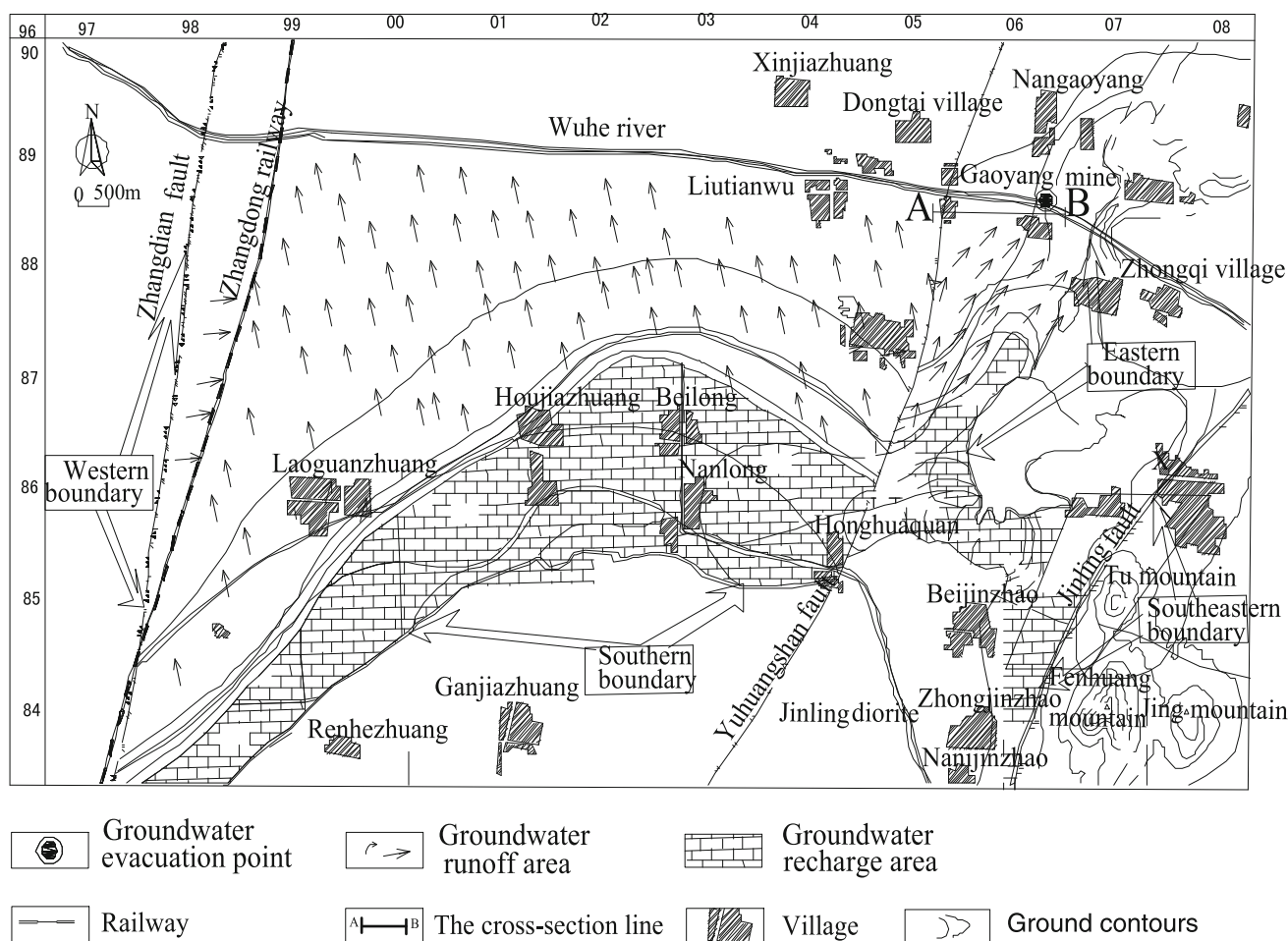
The Basic Principle of Electromagnetic Wave CT Cross-hole Detection

The technique of tomography is a method of image reconstruction, an application of image processing that has been widely applied in astronomy, biology, medicine, and

geology (Luo 2005). Its mining-related application involves a controllable emission source (a symmetrical dipole that transmits with a frequency between about 0.5 and 32 MHz) in a borehole and whip antenna receivers in other boreholes that detect the amplitude of the emitted radiation density. The physical distributions of underground media absorb electromagnetic energy differently based on various factors, such as fractures, water volume, mineral composition, and lithology (Guo and Wei 1999). By comparing the deviation

Table 2 Hydrogeological conditions of the Gaoyang iron mine area

Boundary	Geologic structure	Hydrogeological conditions
West	Zhangdian fault	The Zhangdian fault is a compresso-shear reverse fault; its west side is Jurassic and Cretaceous and east side is Ordovician. The fault does not form a hydraulic boundary
East	Jinling fault	The East Jinling fault is a compresso-shear fault, with a very smashed core; it is almost filled by white clay so it has very limited permeability. Therefore, the Jinling fault can be considered water resistant boundary of the East mine area
Southeast	Jinling diorite intrusive body	The diorite rock has little permeability and porosity, and so has limited water-burst potential. It cuts off the direct hydrologic connection between the inner and outer limestone ground water associated with the area, forming a water-resistant boundary southeast of the mine area
South	Ordovician limestone	The area of Ordovician limestone emergence can directly receive rainfall as groundwater as it is in direct contact with the Quaternary sand and gravel, leading to the possibility of a hydrodynamic connection with the Quaternary system water


Fig. 4 Schematic groundwater movement (arrows) in Ordovician limestone in Gaoyang Iron Mine

between the emitted and received signals, a structural image can be constructed between the boreholes (Feng et al. 1995). The amplitude attenuation of the electromagnetic wave can be expressed by applying an optical approximation (Yue 2007):

$$E = E_0 \exp \left[- \int R \beta(r) dr \right] f/R \quad (1)$$

where E_0 is the amplitude of the wave emitted, R is the distance between the emission point and the receiving

point, f is the directivity, β is the absorbing index of the media in the explored region, and E is the detected amplitude of the field density at the receiving location. Equation 1 shows that E_0 is attenuated to E . β is affected by the permeability of the media, but also by the electrical resistivity, ρ , the dielectric constant, ε , and the electromagnetic wave frequency, ω . When ω and μ are constant, β is inversely related to ρ . Thus, the absorbing index of the media is indicative of the nature of the rock mass.

Detection of the Groundwater Flow Channels Using Electromagnetic Wave CT

The roadway layout at the -285 m level of the Gaoyang deposit is shown in Fig. 5. In 2009, about 7,000–8,000 m^3/d of water flowed from the west at this level. The locations of four monitoring boreholes (KT09, KT10, KT11, and KT12), which are in the western section of the -245 m level, are shown in Fig. 5.

In this application, the electromagnetic wave CT detection was operated in the return airway at the -245 m level, using a working frequency between about 4 and 12 MHz. The transmitting and receiving antennas were arranged at fixed distances, approximately 25 m apart. Abnormal bodies such as cavities and shattered fault zones of $<1 \text{ m}^3$ could be detected. The sectional CT figures identified six areas with abnormal EW (electromagnetic wave) absorption. Explanations of the results are as follows:

1. The absorption coefficient β of the three sections were different: β in KT10–KT11 was greater than that of the other two sections, which indicated that the degree of fragmentation of the corresponding rock formation was higher in this section. According to the identification of the core obtained from drilling KT10 and KT11, this is due to a shattered fault zone between the KT10 and KT11 holes. At about the -270 to -275 m level of the cross section, there were some areas with relatively high β values, which indicated possible faulted areas.
2. Exploration and interpretation of the KT9–10 sectional figures: β was measured as 1.8–3.0 dB/m for the -265 m level and above, and 3.0–4.6 dB/m below this level. There were two obvious high absorption coefficient abnormal areas: Areas I and II. These two areas showed abnormally high β (3.8 dB/m up to 4.6 dB/m) in a certain area. Based on the core obtained from drilling KT9, it was concluded that these areas contain extensively developed karst voids and abundant water. Furthermore, there was some scattered and uncorrelated abnormally high β value areas in the deepest part of this section, which indicate small cavities filled with water.
3. Exploration and interpretation of the KT10–11 sectional figures: β was about 3.6 dB/m above the -290 m level, greater than that of the other two sections, while at lesser well depths, there were two abnormal areas (areas III and IV) with high absorption coefficients and elevated β coefficients, ranging from 4.6 to 5.8 dB/m. The abnormality in Area IV had some degree of inclination toward KT10. Based on the known information, it was concluded that these areas are shattered fault zones and karst cavities that contain water.
4. Exploration and interpretation of the KT11–12 sectional figures: there was a high elevation area at the -260 m level shaped like an inverted triangle, with $\beta \approx 3.8$ dB/m, which indicated that the rock mass integrity there is poor. Between -260 and -288 m, β was relatively low, within 1.8–3.0 dB/m, indicating better rock mass integrity. At the -288 m level, there were two areas with abnormally high absorption coefficients and abnormally high relative β , from 4.2 dB/m up to >5.0 dB/m. Based on known information, it was concluded that karst is highly developed in these areas and that it contains abundant water.

A CT graph of the β distribution was obtained through inverse derivation. Lower values of β indicate less absorption of the electromagnetic wave by the medium, and better medium integrity (Yue 2007). So, where the absorption coefficient is low ($\beta = 2.2\text{--}3$ dB/m), the integrity of the medium is good; a moderate absorption coefficient ($\beta = 3\text{--}3.8$ dB/m) means that the integrity of the medium is fair; a high absorption coefficient ($\beta > 3.8$ dB/m) is generally caused by karst caves, cracks, and shattered fault zones. By combining the three section figures into a synthesized profile (Fig. 6), the correlation between the different abnormal areas was identified. Areas II and III and Areas IV and V were connected. The results showed that the groundwater inrush channel of the Gaoyang deposit is caused by cavities and faults at the -283 m level. Blocking the groundwater inrush channel should be the key to prevention and control of water inrushes into the deposit.

Monitoring of the Groundwater Level and Curtain Grouting Treatment and Blocking

Analysis of the Groundwater Level Monitoring

The groundwater level data from boreholes KT9 and KT10 from Dec. 1, 2008 to March 10, 2009 and from July 29, 2009 to Dec. 6, 2009 are graphed on Fig. 7. The groundwater

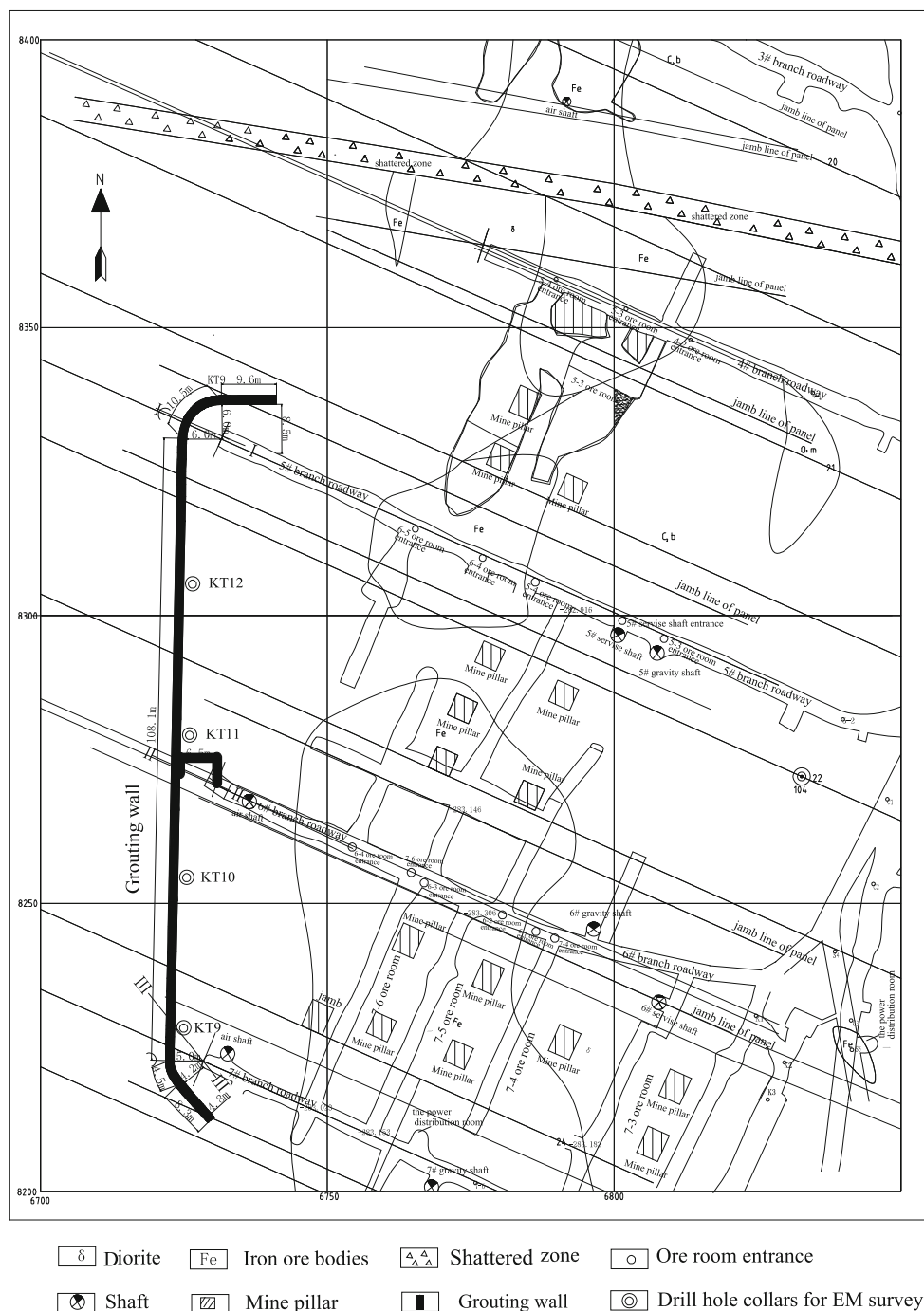


Fig. 5 Drill hole pattern for electromagnetic (EM) survey and curtain grouting curtain at the -285 m level of Gaoyang Iron Mine

elevation of KT9 is always higher than that of KT10, which shows that the southwest side of the mine has the higher groundwater level and suggests that the groundwater flows from southwest to northeast (from KT9 to KT10). This analysis is supported by the consistent pattern displayed by the water levels and pressures at the discharging holes at each branch roadway.

The Grouting Design of the Gaoyang Iron Mine

By injecting slurry into a rock fracture, a man-made underground watertight grout curtain can be formed to cut off a water channel and create a dry environment in the mine area. Based on the groundwater level monitoring data and the CT results, it was decided that the hydraulic

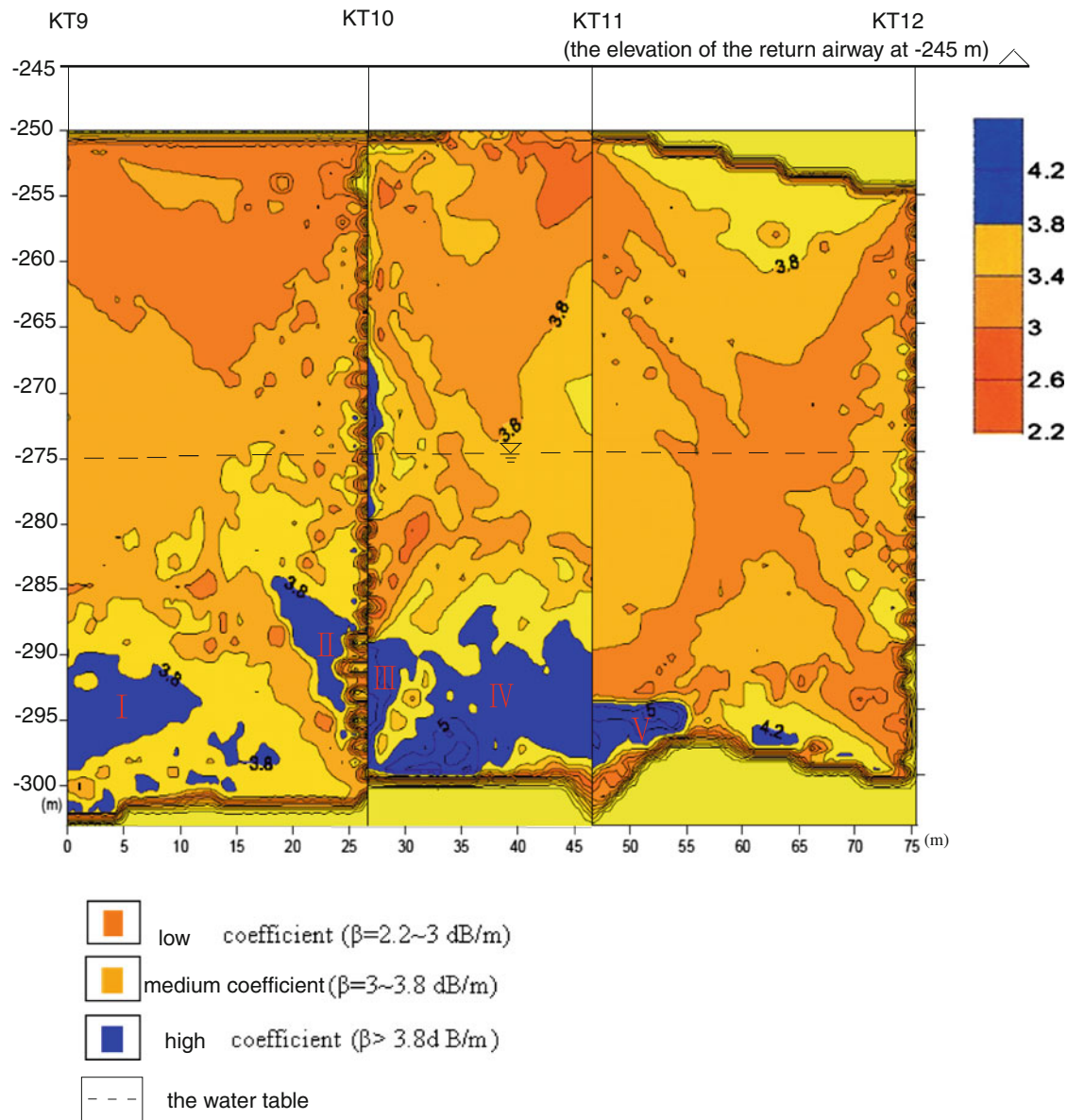


Fig. 6 Isoline diagram of β , apoxy for permeability and electrical resistivity, in a vertical plane through bore holes KT9-12

channels in the area with high groundwater levels, in the southwestern side of the mine, should be grouted and groundwater level monitoring should be implemented in the area with low water levels. Grouting was principally focused in the area between 5# and 7# branch roadways, at depths ranging from -270 to -285 m.

The designed grouting pressure in the fractured rock mass and the grouting thickness was determined in terms of the fractured rock mass grouting pressure and curtain borehole design empirical formula (Eqs. 2, 3) (Liu and Wang 2008).

$$p_e = p_w + \gamma \cdot H + m(H_1 - H) - (H_1 \cdot \gamma_G - S \cdot \gamma_w) \quad (2)$$

where p_e is the designed grouting pressure; p_w is the hydrostatic pressure of groundwater; γ is the density of

covering layer above grouting segment, γ_G is the density of slurry, H is the thickness of the layer above slurry stop; and H_1 is the total thickness of grouting segment. A grout thickness of 1.8 m can be produced using a curtain diffusion radius of 1.75 m and a length between the adjoining boreholes of 3.0 m:

$$l = 2 \cdot \sqrt{r^2 - \frac{T^2}{4}} \quad (3)$$

where T is a grout thickness, r is a curtain diffusion radius, and l is the length between the adjoining boreholes. Therefore, according to the grouting parameters above, the terminal jet grouting diffusion radius of borehole grouting was fixed at 1.75–2.50 m. A total of 174 boreholes were used for grouting, to produce a seepage prevention curtain wall that is

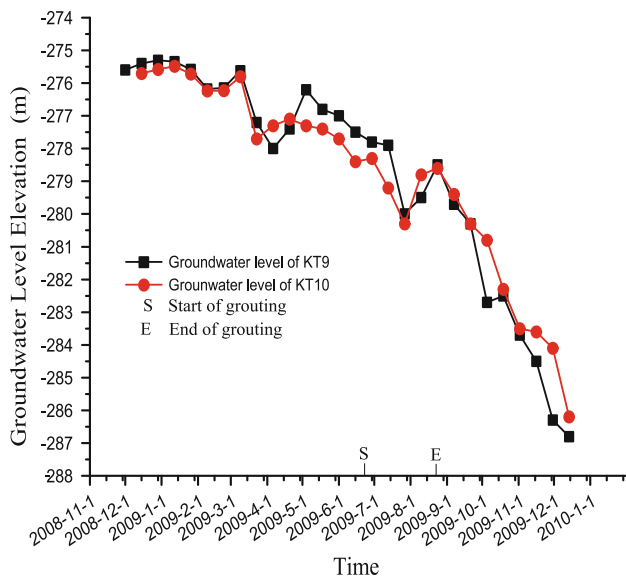


Fig. 7 Graph of groundwater level elevation with time

141 m long, 15 m high, and about 1.8 m thick, to keep groundwater outside of the southwestern section of the mine area. The distribution of the grout curtain wall and the section of curtain grouting construction can be seen in Figs. 5 and 8.

The water inrush channel grouting project at the –285 m level of Gaoyang Iron Mine was completed on Aug. 22, 2009. The changes of groundwater level and the water yield after the implementation of the blocking by grouting in the mine area are shown in Fig. 7. As shown in Fig. 7, the groundwater level of the mine area declined

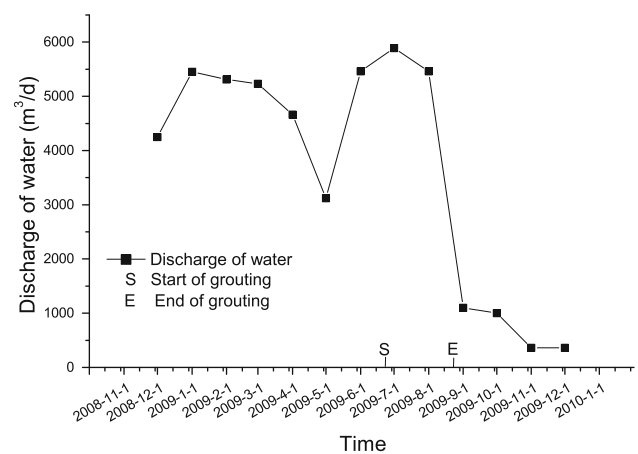


Fig. 9 Daily discharge of water with time at Gaoyang Iron Mine

slowly from –275 to –278 m from Jan. 2009 to the end of June 2009. In Sept. 2009, after grouting was completed, the groundwater level of the mine area declined significantly, from –278 m before grouting to –286 m now, which means that the groundwater level has declined beneath the lowest extraction level.

Figure 9 shows that before grouting from Jan. 2009 to Aug. 2009, the daily discharge of mine water ranged between 3,000 and 6,000 m³/d. After grouting, the daily discharge declined rapidly, from about 6,000 m³/d in July 2009 to about 1,000 m³/d in Sept. 2009. The average daily discharges of water in 2010 and 2011 have fallen below 200 m³/d, which has eliminated the threat created by the high groundwater pressure in all of the ore bodies and

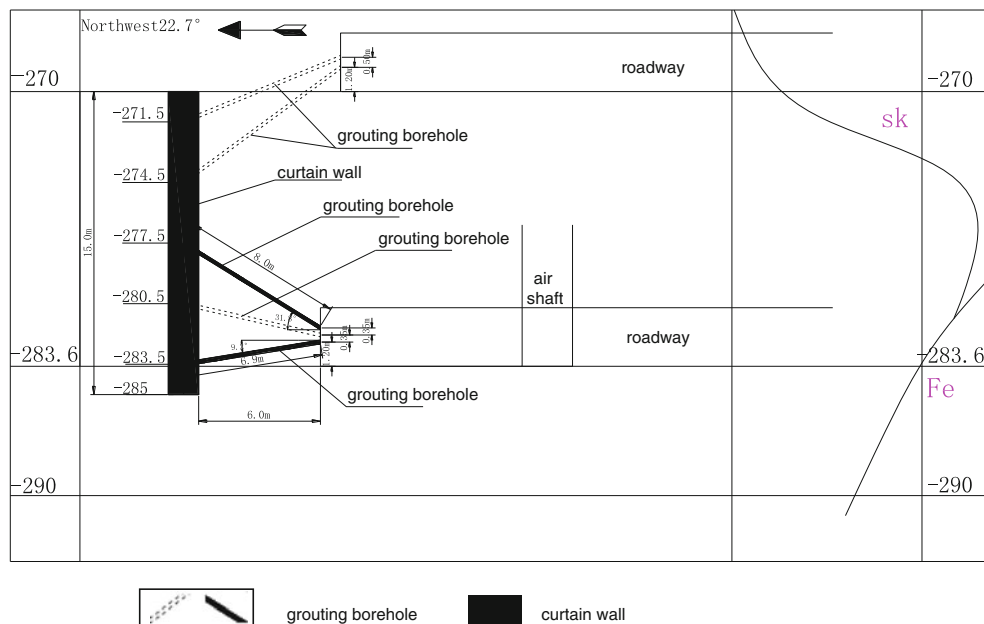


Fig. 8 The section of curtain grouting construction

should allow exploitation in a low water pressure environment. It has also saved a lot of money previously spent pumping water from the mine and guaranteed safe, regular production at the Gaoyang Iron Mine.

Conclusions

1. Groundwater in the Ordovician limestone is the biggest threat to the Gaoyang Mine. Exploitation of the Gaoyang deposit allowed this water access to the mine, which led to the groundwater inrush events. The abundant groundwater of the Ordovician limestone flows from the south and west of the Gaoyang deposit through karst (caves) and faults.
2. The use of computerized borehole tomography allowed the authors to explore the hydrogeological conditions of the main hydraulic channel and to locate the connecting karst cavities and faults below the –283 m level west of the deposit. The size, distribution, and connectedness of the channel were also confirmed. A curtain wall grouting plan was developed and executed.
3. Monitored groundwater levels and CT assessments at the Gaoyang Iron Mine indicate that the groundwater inrush channels in the high water level areas in south and west of the mine area have been effectively blocked off. Groundwater levels are now being monitored in the low water level areas to detect any changes that might develop over time, but at present, it appears that the grouting has effectively eliminated the threat of high groundwater pressure inrush events for all the ore bodies.

Acknowledgments The research discussed in this article was sponsored by the Open Research Foundation of Water Resources and

Hydropower Research of China (IWHKRF 2010119) and the Special Research Foundation of the Doctoral Program of the Ministry of Education (No. 20113721110002). Many thanks for the accurate geological information and the help provided by the production know-how personnel, including Mr. Bai Jianye, Mr. Li Qingqian, Mr. Fu Zenghua, and Mr. Xie Zhifeng. Thanks also for the data provided by the Tai'an Dingxin Geography CT Detection Company during the electromagnetic wave CT detection.

References

- Bao WM, Fan JX, Yang JM (2009) Research on rainwater utilization of Zibo city. *J Shandong Normal Univ* 4:84–87 (in Chinese)
- Feng R, Zhou HN, Tao YL, Zhang JT (1995) Application of electromagnetic tomography in fractured zones prospecting. In: *Proceedings of the 3rd SEGJ/SEG international symposium, geotomography—fracture imaging*, Tokyo, Japan
- Guo G, Wei BL (1999) Prospecting corroded cavities using cross-section electromagnetic tomographic technique between boreholes. *S Chin J Seismol* 19(4):30–34 (in Chinese)
- Li MZ, Wang JH, Tie PJ (2006) A study of the mechanism of water inrush and prevention measurements of the bauxite aluminium ore in Jiagou. *Henan Hydrogeol. Eng Geol* 33(85–89):94
- Liu WY, Wang XG (2008) *Grouting materials and construction technology*. China Building Materials Press, Beijing (in Chinese)
- Luo YX (2005) The cross-well electromagnetic computerized tomography technology and its application in the cavern survey. *Detect Eng (Geotech Drill Eng)* 10:28–29 (in Chinese)
- Wang XB (2005) Research on mining technology for Gaoyang iron mine under complex hydrogeological conditions. *Metal Mine* 7:10–13, 16 (in Chinese)
- Yue CW (2007) Study on the cross-well electromagnetic tomography and its application. MS thesis, Jilin University, Changchun, China (in Chinese)
- Zhang FW (1989) Analysis of the groundwater system of Zibo Basins. The collected works of hydrogeological engineering, Geological Institute of the Chinese Academy of Geology Sciences 5 (in Chinese)